





Thermoelectrohydrodynamic convection in parallel plate capacitors under dielectric heating conditions

Harunori N. Yoshikawa ^{*}



Université Côte d'Azur, CNRS, Institut de Physique de Nice, 06100 Nice, France

Changwoo Kang [†] and Innocent Mutabazi 

Normandie Université, UNIHAVRE, CNRS UMR 6294, Laboratoire Ondes et Milieux Complexes, 53 Rue de Prony, CS 80540, 76058 Le Havre Cedex, France

Florian Zaussinger 

Faculty Applied Computer Sciences and Biosciences, Mittweida University of Applied Sciences, Technikumplatz 17, 09648 Mittweida, Germany

Peter Haun  and Christoph Egbers 

Department of Aerodynamics and Fluid Mechanics, Brandenburg University of Technology Cottbus-Senftenberg, Siemens-Halske-Ring 14, D-03046, Cottbus, Germany



(Received 8 June 2020; accepted 20 October 2020; published 13 November 2020)

The thermal convection of dielectric fluid in an alternating electric field is investigated by the linear stability theory. We consider fluid layers confined in parallel plate capacitors without any externally imposed temperature difference. Only the internal heating by dielectric loss generates temperature gradients. The thermal variation of fluid permittivity induces electrical heterogeneity in the fluid and results in the dielectrophoretic (DEP) force, which can drive the convective motion of fluid. Assuming electric fields of high frequency, we develop a theoretical model to describe the flow dynamics under dielectric heating. For simplicity, the capacitor is placed either in microgravity environments or in a horizontal configuration on the earth. We determine the critical conditions for the DEP force to overcome stabilizing diffusion effects for convection generation. All the analyses are performed in the light of the similarity between the DEP force and the thermal Archimedean buoyancy, introducing an effective electric gravity. Examining energy transfer processes to convection flow, we confirm that the driving mechanism of convection in microgravity is similar to the ordinary thermal convection but in an electric effective gravity except for a stabilizing thermoelectric feedback effect. In the horizontal configuration, we show that the competition of the electric gravity with the earth's gravity affects the critical conditions and enriches the flow patterns of the resulting convection.

DOI: [10.1103/PhysRevFluids.5.113503](https://doi.org/10.1103/PhysRevFluids.5.113503)

I. INTRODUCTION

Flows induced by electrohydrodynamic (EHD) effects have been investigated widely to generate and control the motion of dielectric and electrically poorly conducting fluids [1,2]. Different flow

^{*}Harunori.Yoshikawa@univ-cotedazur.fr

[†]Present address: Department of Mechanical Engineering, Jeonbuk National University, 567 Baekje-daero, Deokjingu, Jeonju-si, Jeollabuk-do, 54896, Republic of Korea.

generation mechanisms have been explored to enhance mass, momentum, and heat transport by applying electric fields [3]. Coulomb forces on free charges in fluid are used to generate fluid motion for EHD mixing devices and electroosmotic pumps [2]. Forces resulting from polarization of fluid molecules are also used to drive fluid motion. Differential polarization of fluid leads to a net body force. The dielectrophoresis, which is a technique to transport polarizable particles in dielectric fluid, explores this effect [4]. A dielectrophoretic (DEP) micromixer was proposed [5], in which dielectric microparticles suspended in fluid are agitated by an electric field to enhance mixing. Even in the absence of suspended particles, the dielectrophoretic effect can induce motion in a pure fluid. For example, the thermal variation of fluid permittivity results in a DEP force aligned with the temperature gradient to generate a thermal convection, called thermoelectrohydrodynamic (TEHD) convection [3].

The EHD force per unit volume is given by

$$\mathbf{f}_{\text{EHD}} = \rho_e \mathbf{E} - \nabla \left[\frac{\rho}{2} \left(\frac{\partial \epsilon}{\partial \rho} \right)_T \mathbf{E}^2 \right] - \frac{\mathbf{E}^2}{2} \nabla \epsilon, \quad (1)$$

for an isotropic linear dielectric fluid, where \mathbf{E} is the electric field, ρ_e is the density of free charges, ρ and ϵ are the mass density and permittivity of fluid, and T denotes the temperature of fluid [6]. The first and second terms on the right-hand side are the Coulomb force on free charges and the electrostrictive force component, respectively. The third term represents dielectrophoretic effects and will be denoted by \mathbf{f}_D . For a small temperature deviation θ from a reference T_{ref} , i.e., $\theta = T - T_{\text{ref}}$, the permittivity of a fluid of uniform chemical composition can be modeled by a linear equation of state:

$$\epsilon = \epsilon_{\text{ref}}(1 - e\theta), \quad (2)$$

with a thermal coefficient e , which takes a value of order 10^{-2} to 10^{-3}K^{-1} typically [7,8]. The permittivity at the reference temperature T_{ref} has been denoted by ϵ_{ref} .

The TEHD convection has been investigated since the late 1960s [9,10], motivated particularly by the analogy of dynamical effects of \mathbf{f}_D and those of the thermal Archimedean buoyancy force \mathbf{f}_{Ar} . The latter is given by $\mathbf{f}_{\text{Ar}} = -\rho_{\text{ref}}\alpha\theta\mathbf{g}$ for small temperature deviations, where ρ_{ref} is the density of fluid at the reference temperature and α is the coefficient of thermal expansion. In fact, the rate of vorticity generation by the DEP force is $\nabla \times \mathbf{f}_D = \nabla \times [-(\mathbf{E}^2/2)\nabla\epsilon] = \epsilon_{\text{ref}}e\nabla(\mathbf{E}^2/2) \times \nabla\theta$. This result is the same as the vorticity generation rate by the Archimedean force, $\nabla \times \mathbf{f}_{\text{Ar}} = \rho_{\text{ref}}\alpha\mathbf{g} \times \nabla\theta$, once the earth's gravitational acceleration \mathbf{g} is replaced by the following effective gravity,

$$\mathbf{g}_e = \frac{e}{\rho_{\text{ref}}\alpha} \nabla \left(\frac{\epsilon_{\text{ref}}\mathbf{E}^2}{2} \right). \quad (3)$$

The effects of \mathbf{f}_D on flow generation in incompressible fluids can therefore be understood intuitively by regarding the force \mathbf{f}_D as a thermal buoyancy force in the electric effective gravity \mathbf{g}_e . Thermal convection inside planets, e.g., the mantle convection in the earth, could be simulated by the TEHD convection in a central effective gravity \mathbf{g}_e realized in *either* spherical *or* cylindrical capacitors [11,12].

Experiments on the TEHD convection have been performed in curved geometries because of geophysical interests [8,11,13,14] rather than in plane geometries [10]. In TEHD experiments, microgravity conditions are often used to avoid the effects of the thermal Archimedean buoyancy. An early experiment in a hemispherical capacitor was performed during the SpaceLab 3 mission in 1986 [13]. A series of experiments in a spherical capacitor have been carried out recently on board the International Space Station [8,15] during the *GeoFlow* mission. Complex structures of the convective flow in the central force field have been revealed through flow visualization by Wollaston prism shearing interferometry [16]. The results were compared with numerical simulations [17,18]. Further experimental investigations by a similar apparatus are planned in the scope of the *AtmoFlow* experiment [19]. Experiments were also performed in cylindrical capacitors subject to a radial

temperature gradient on the ground [11] and in microgravity environments during parabolic flight campaigns [14,20]. The latter experiments have revealed convection cells generated by the DEP force \mathbf{f}_D .

Results of investigations on the TEHD convection are often described in terms of a Rayleigh number L based on the electric gravity because of the analogy:

$$L = \frac{\alpha \Delta T \|\mathbf{g}_e\| l^3}{\nu \kappa}, \quad (4)$$

where ΔT and l are the characteristic temperature difference and the characteristic length of a given fluid system. The kinematic viscosity and the thermal diffusivity of fluid have been denoted by ν and κ , respectively. For stationary dielectric fluid-filling parallel plate capacitors subject to an externally imposed temperature difference ΔT , the linear stability theory predicts convective flows when L exceeds a critical value of $L_c = 2128.7$ [7,9,10,21]. As shown by a detailed theoretical analysis [21], the generation mechanism of the TEHD convection is similar to that of the natural convection except for a stabilizing thermoelectric feedback effect. The critical Rayleigh number of the TEHD instability larger than that of the Rayleigh-Bénard instability (1708) is explained from this stabilizing effect.

All the existing theoretical and numerical investigations on the TEHD convection, however, consider perfect dielectric fluids and neglect dielectric loss except recent numerical studies in spherical geometries [22–24]. This assumption would be a good approximation for nonpolar dielectrics that have a small loss tangent ($\tan \delta$) under typical experimental conditions. For polar fluids, however, the polarization occurs with a phase delay. The displacement current $\mathbf{j}_D = \partial \mathbf{D} / \partial t$ then produces thermal energy inside fluid, where \mathbf{D} is the electric displacement field and t denotes the time. Its power is given by

$$\overline{P_D} = \overline{\mathbf{j}_D \cdot \mathbf{E}} = \omega \epsilon'' \overline{\mathbf{E}^2}, \quad (5)$$

per unit volume, where ω is the angular frequency of field. The coefficient ϵ'' is the imaginary part of the complex permittivity $\hat{\epsilon} = \epsilon' - i\epsilon''$ and is related to the real part ϵ' by the loss tangent, $\epsilon'' = \epsilon' \tan \delta$. The overline stands for the average over an oscillation period of electric field: $\overline{(\bullet)} = (\omega/2\pi) \int_t^{t+2\pi/\omega} (\bullet) dt$. The significance of heat generation on fluid temperature fields can be estimated by a dimensionless number \mathcal{Y} comparing the heat generation with the diffusion of thermal energy [12], $\mathcal{Y} = \omega \epsilon' \tan \delta E^2 l^2 / \lambda \Delta T$, wherein E is a characteristic value of the electric field and λ is the thermal conductivity of fluid. Silicone oils less viscous than $10^{-4} \text{ m}^2/\text{s}$ are often used in experimental investigations. The loss tangents of these oils are of the order 10^{-4} in a frequency range of 10^2 to 10^7 Hz. The number \mathcal{Y} takes a value of the order 10^{-2} when $E \sim 10^6 \text{ V/m}$, $\omega/2\pi \sim 10^2 \text{ Hz}$, $\Delta T \sim 1 \text{ K}$, and $l \sim 10^{-2} \text{ m}$. It justifies the assumption of perfect dielectrics. In some polar fluids, the dielectric tangent takes large values. For 1-nonanol, which was used in a GeoFlow experiment [25], $\tan \delta = 0.06$ and $\mathcal{Y} \sim 2$ under the same thermal and electrical conditions. The dielectric heating will then affect the flow dynamics. Indeed, Zaussinger *et al.* [22] demonstrate by a numerical simulation that TEHD convection develops due to dielectric heating in 1-nonanol without any externally applied temperature gradient.

In the present work, we investigate the TEHD instability in fluids heated internally due to dielectric loss. We develop a theoretical model to include the effects of dielectric heating on the flow dynamics. To focus on the instability provoked by internal heating, we consider the stability problem in parallel plate capacitors with an infinite lateral extension and without any external source of the temperature gradient (Fig. 1). In Sec. II, a theoretical model is presented and its validity conditions are discussed. The quiescent state of fluid is determined from the model. We then introduce a set of dimensionless numbers, nondimensionalizing the governing equations. A linear stability analysis is performed for this base state in Sec. III. Obtained results are presented in Secs. IV and V, first for capacitors in microgravity environments and then for horizontal capacitors. For each of these configurations the energy transfer mechanism from the base to perturbation flows is examined. The

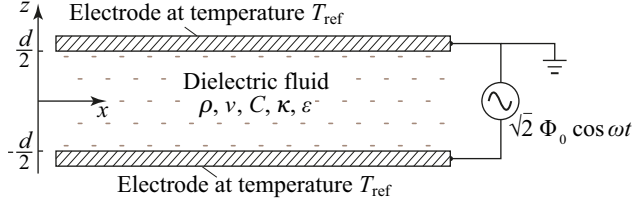


FIG. 1. Geometrical configuration of the problem.

results on the stability are confronted with thermal instabilities in superposed immiscible fluid layers and in internally heated single layers in Sec. VI. Concluding remarks are given in Sec. VII.

II. THEORETICAL MODEL

The TEHD convection can be generated only when alternating electric fields of high frequencies are applied to fluids of small electrical conductivity. Otherwise, the Coulomb forces on free charges have dominant effects over flow dynamics even in initially electroneutral fluids. In fact, the accumulation of free charges can occur inside fluids under low-frequency fields to induce fluid motion, as observed in Melcher-Taylor pumping [26,27]. For the forces on free charges to be negligible, the frequency of the field should be high compared to the reciprocals of the timescales of the momentum and thermal diffusion processes and the timescales characterizing the motion of free charges [28]:

$$\omega \gg \tau_v^{-1}, \tau_\kappa^{-1}, \tau_e^{-1}, \tau_m^{-1}, \tau_d^{-1}, \quad (6)$$

where $\tau_v = d^2/\nu$ is the viscous time and $\tau_\kappa = d^2/\kappa$ is the thermal diffusion time. The timescales τ_e , τ_m , and τ_d are of the charge relaxation, migration, and diffusion processes, respectively. Under the condition (6), the electric field oscillation is much faster than the temporal evolution of the velocity and temperature fields and of the electric charge distribution. The Coulomb forces on free charges then cancel out over a period of electric field [3]. Only the time-averaged component of the DEP force, $\overline{\mathbf{f}_D}$, and the averaged dielectric heating, $\overline{P_D}$, can affect the fluid motion and the temperature field. Most of existing theoretical and numerical studies on the TEHD convection suppose the high-frequency condition (6) to model the dynamics of dielectric fluids only with time-averaged EHD effects [7,9,10,21,29]. Smorodin and Velarde examine the parametric excitation of dielectric fluid by time-varying DEP force [30]. Their results confirm that the use of time-averaged EHD forces in the analysis of the TEHD instability is valid when $\omega\tau_v \gtrsim 100$. In the experimental studies [8,10,11,13,14], electric fields of a frequency of $\sim 10^2$ – 10^4 Hz were applied to dielectric fluid layer for fulfilling the condition (6).

A. Governing equations

For small temperature variation, fluids are effectively incompressible and the flow dynamics can be modeled by the Oberbeck-Boussinesq approximation for EHD flows [10]. The governing equations then consist of the mass, momentum, and heat-conduction equations and of the Faraday and Gauss laws for electricity:

$$\nabla \cdot \mathbf{u} = 0, \quad (7a)$$

$$\rho_{\text{ref}} \left(\frac{\partial \mathbf{u}}{\partial t} + \mathbf{u} \cdot \nabla \mathbf{u} \right) = -\nabla p_r + \rho_{\text{ref}} \nu \nabla^2 \mathbf{u} - \rho_{\text{ref}} \alpha \theta \mathbf{g} + \overline{\mathbf{f}_D}, \quad (7b)$$

$$\rho_{\text{ref}} C \left(\frac{\partial \theta}{\partial t} + \mathbf{u} \cdot \nabla \theta \right) = \lambda \nabla^2 \theta + \overline{P_D}, \quad (7c)$$

$$\nabla \times \hat{\mathbf{E}} = \mathbf{0}, \quad (7d)$$

$$\nabla \cdot [(\epsilon' - i\epsilon'')\hat{\mathbf{E}}] = 0, \quad (7e)$$

where \mathbf{u} is the velocity field and p_r is a reduced pressure: $p_r = p + \rho gz + \rho(\partial\epsilon/\partial\rho)_T \overline{\mathbf{E}}^2/2$. The specific heat of fluid at constant pressure is denoted by C . The complex electric field $\hat{\mathbf{E}}$ defined as $\mathbf{E} = \text{Re}[\sqrt{2}\hat{\mathbf{E}}(t, \mathbf{r})e^{i\omega t}]$ has been introduced. The symbol $\text{Re}[\cdot]$ means the real part of a complex number. The time dependence of $\hat{\mathbf{E}}$ represents the variation of the electric field via the temporal evolution of temperature θ , which will occur over a timescale much larger than the period of electric field oscillation ($2\pi/\omega$) according to the high-frequency hypothesis (6). The equation of state (2) reads as follows for the complex permittivity $\hat{\epsilon} = \epsilon' - i\epsilon''$:

$$\epsilon' = \epsilon'_{\text{ref}}(1 - e'\theta), \quad \epsilon'' = \epsilon''_{\text{ref}}(1 - e''\theta), \quad (8)$$

where e' and e'' are the coefficients of thermal permittivity variation. We refer to the latter coefficient as e_r rather than as e'' itself, introducing the ratio of the two coefficients $e_r = e''/e'$.

The DEP force $\overline{\mathbf{f}}_D$ in Eq. (7b) is calculated from the complex electric field $\hat{\mathbf{E}}$ (see Appendix A):

$$\overline{\mathbf{f}}_D = -\frac{1}{2}\{(\hat{\mathbf{E}} \cdot \hat{\mathbf{E}}^*)\nabla\epsilon' + i\epsilon''[(\nabla\hat{\mathbf{E}}^*) \cdot \hat{\mathbf{E}} - (\nabla\hat{\mathbf{E}}) \cdot \hat{\mathbf{E}}^*]\}, \quad (9)$$

where an asterisk means the complex conjugate. Substituting the equations of state (8) in Eq. (9), we obtain the following expression of DEP force:

$$\overline{\mathbf{f}}_D = \nabla\left(\frac{\epsilon'_{\text{ref}}\hat{\mathbf{E}} \cdot \hat{\mathbf{E}}^*}{2} e'\theta\right) - \rho_{\text{ref}}\alpha\theta\mathbf{G}_e + \mathbf{f}_R, \quad (10a)$$

with

$$\mathbf{G}_e = \frac{\epsilon'_{\text{ref}}e'}{2\rho_{\text{ref}}\alpha}\{\nabla(\hat{\mathbf{E}} \cdot \hat{\mathbf{E}}^*) - ie_r \tan\delta[(\nabla\hat{\mathbf{E}}^*) \cdot \hat{\mathbf{E}} - (\nabla\hat{\mathbf{E}}) \cdot \hat{\mathbf{E}}^*]\}, \quad (10b)$$

$$\mathbf{f}_R = -\frac{i\epsilon'_{\text{ref}}\tan\delta}{2}[(\nabla\hat{\mathbf{E}}^*) \cdot \hat{\mathbf{E}} - (\nabla\hat{\mathbf{E}}) \cdot \hat{\mathbf{E}}^*]. \quad (10c)$$

The first term on the right-hand side of Eq. (10a) is a potential force and has no dynamical effect on flow generation inside incompressible fluids. The second term is the thermoelectric buoyancy force, which is the analog to the thermal Archimedean buoyancy force. The generalized electric gravity \mathbf{G}_e retrieves Eq. (3) in the limit of vanishing $\tan\delta$. The third term \mathbf{f}_R is a residual component of the DEP force. The dynamical effects of \mathbf{f}_R cannot be assimilated as a thermal buoyancy force in an effective gravity field.

Equations (7) and (10) give a set of governing equations describing fully the dynamics of dielectric fluid flows subjected to dielectric heating, once completed by the following dielectric heating formula derived from Eq. (5):

$$\overline{P}_D = \omega\epsilon''_{\text{ref}}(1 - e_r e'\theta)\hat{\mathbf{E}} \cdot \hat{\mathbf{E}}^*. \quad (11)$$

To handle electric fields, however, it is convenient to introduce the electric potentials ϕ and ψ , allowed by the Faraday law [Eq. (7d)], and to transform the Gauss law [Eq. (7e)] into another form. The potentials are both real functions and related to the complex electric field by $\hat{\mathbf{E}} = -(\nabla\phi + i\nabla\psi)$. Making use of these potentials and separating the real and imaginary parts of Eq. (7e), we obtain

$$(1 - 2e'F_+\theta)\nabla^2\phi - e'F_+\nabla\theta \cdot \nabla\phi + e'F_-\nabla\theta \cdot \nabla\psi = 0, \quad (12a)$$

$$(1 - 2e'F_+\theta)\nabla^2\psi - e'F_-\nabla\theta \cdot \nabla\phi - e'F_+\nabla\theta \cdot \nabla\psi = 0, \quad (12b)$$

where $F_+ = (1 + e_r \tan^2\delta)/(1 + \tan^2\delta)$ and $F_- = (1 - e_r) \tan\delta/(1 + \tan^2\delta)$ have been introduced for brevity. We use this set of equations in the place of Eq. (7e) to determine electric fields.

B. Base quiescent state

We apply the theoretical model presented in Sec. II A to a parallel plate capacitor (Fig. 1) either in microgravity environments or in a horizontal configuration. A high-frequency alternating electric

voltage $\sqrt{2} \Phi_0 \cos \omega t$ is imposed on the capacitor. To focus on flows induced by dielectric heating we consider a capacitor without any externally imposed temperature gradient. Both electrodes are then maintained at the same temperature T_{ref} . For simplicity the lateral extension of the capacitor is assumed to be large enough to neglect any perturbation induced by lateral walls.

This fluid system is invariant with respect to rotation around any axis perpendicular to the electrodes and to translation in any direction parallel to the electrodes. When the applied electric voltage is small, the fluid system will respect these symmetries and be in a quiescent state, $\mathbf{u} = 0$. The temperature and electric fields vary only in the perpendicular direction: $\mathbf{u} = 0$, $\theta = \theta_b(z)$, $\phi = \phi_b(z)$, and $\psi = \psi_b(z)$. The heat conduction equation (7c) and the Gauss law (12) read as follows:

$$\lambda \frac{d^2 \theta_b}{dz^2} + \omega \epsilon'_{\text{ref}} (1 - e_r e' \theta_b) \left[\left(\frac{d\phi_b}{dz} \right)^2 + \left(\frac{d\psi_b}{dz} \right)^2 \right] = 0, \quad (13a)$$

$$(1 - 2e' F_+ \theta_b) \frac{d^2 \phi_b}{dz^2} - e' F_+ \frac{d\theta_b}{dz} \frac{d\phi_b}{dz} + e' F_- \frac{d\theta_b}{dz} \frac{d\psi_b}{dz} = 0, \quad (13b)$$

$$(1 - 2e' F_+ \theta_b) \frac{d^2 \psi_b}{dz^2} - e' F_- \frac{d\theta_b}{dz} \frac{d\phi_b}{dz} - e' F_+ \frac{d\theta_b}{dz} \frac{d\psi_b}{dz} = 0. \quad (13c)$$

The solution of this set of equations should satisfy the following boundary conditions:

$$\theta_b = 0, \quad \phi_b = \Phi_0, \quad \psi_b = 0, \quad \text{at } z = \frac{d}{2}, \quad (14a)$$

$$\theta_b = 0, \quad \phi_b = 0, \quad \psi_b = 0, \quad \text{at } z = -\frac{d}{2}. \quad (14b)$$

The temperature increase ΔT due to dielectric heating is determined by the equilibrium between the heating power ($\sim \epsilon'_{\text{ref}} \tan \delta \Phi_0^2 / d^2$) and the thermal diffusion ($\sim \lambda \Delta T / d^2$) according to Eq. (13a). As shown later [see Eq. (17a)], the increase can be estimated by

$$\Delta T = \frac{\epsilon'_{\text{ref}} \omega \Phi_0^2 \tan \delta}{8\lambda}. \quad (15)$$

The relative variation of permittivity, $\gamma_e = (\epsilon / \epsilon_{\text{ref}}) - 1$, is thus given by

$$\gamma_e = e' \Delta T = \frac{e' \epsilon'_{\text{ref}} \omega \Phi_0^2 \tan \delta}{8\lambda}. \quad (16)$$

We call this dimensionless number γ_e *thermoelectric parameter*, which represents the significance of thermoelectric coupling [21]. The present study is concerned only with small γ_e for the validity of the equations of state (8). A purely thermal instability, known as *thermal breakdown* of dielectrics [31], will not occur under this assumption (Appendix C).

When the imposed electric voltage is small, the temperature increase and the permittivity variation are both small. The electric field and the dielectric heating are then uniform so that the temperature profile will be parabolic. Indeed, for vanishing γ_e the solution of Eqs. (13a)–(13c) subject to the boundary conditions (14a) and (14b) is given by

$$\theta_b = \frac{\epsilon'_{\text{ref}} \omega \Phi_0^2 \tan \delta}{8\lambda} \left(1 - \frac{4z^2}{d^2} \right) \left\{ 1 + \frac{\gamma_e}{3} \left[F_+ \left(1 - \frac{4z^2}{d^2} \right) - \frac{e_r}{2} \left(5 - \frac{4z^2}{d^2} \right) \right] \right\}, \quad (17a)$$

$$\phi_b = \Phi_0 \left[\frac{1}{2} + \frac{z}{d} + \frac{\gamma_e F_+ z}{3d} \left(1 - \frac{4z^2}{d^2} \right) \right], \quad (17b)$$

$$\psi_b = \Phi_0 \frac{\gamma_e F_- z}{3d} \left(1 - \frac{4z^2}{d^2} \right). \quad (17c)$$

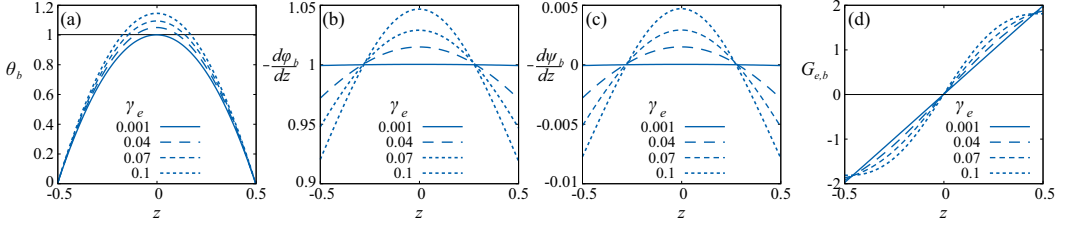


FIG. 2. Base states for some values of the thermoelectric parameter γ_e [Eq. (16)]. Profiles of (a) the temperature θ_b ; (b) the real part of electric field, $-d\phi_b/dz$; (c) the imaginary part of electric field, $-d\psi_b/dz$; and (d) the electric gravity $\mathbf{g}_{e,b} = -G_{e,b}\mathbf{e}_z$. The loss tangent is fixed at $\tan \delta = 0.05$. The temperature, the electric fields, and the electric gravity have been normalized by ΔT , Φ_0/d , and $G_{e,0}$, respectively. See Eqs. (15) and (19) for the definitions of ΔT and $G_{e,0}$.

Any term of an order higher than γ_e^2 has been omitted. The electric gravity $\mathbf{G}_{e,b}$ in the base state is given by

$$\mathbf{G}_{e,b} = -G_{e,b}(z)\mathbf{e}_z, \quad \text{with} \quad G_{e,b} = \frac{8e'\epsilon'_{\text{ref}}\Phi_0^2\gamma_e(1+e_r^2\tan^2\delta)z}{\rho_{\text{ref}}\alpha d^4(1+\tan^2\delta)}, \quad (18)$$

at the leading order. So, the base state is composed of two immobile fluid sublayers of a thickness $d/2$, in each of which the electric gravity is oriented toward the hot core of the capacitor. The density stratification is thus unstable against the thermoelectric buoyancy in each sublayer.

Basic fields for finite values of γ_e are computed from Eqs. (13a)–(13c) by the Chebyshev collocation method (Fig. 2). The fields $(\theta_b, \phi_b, \psi_b)$ are symmetric with respect to the midgap plane $z = 0$, while the acceleration field $G_{e,b}$ has an antisymmetric profile. The profiles of these fields are more deflected for larger γ_e , deviating from the analytical expressions (17). The qualitative relationship between the temperature gradient and the electric gravity is the same as in the case of vanishing γ_e . Both are directed toward the capacitor core. The density stratification in each sublayer is thus unstable against the thermoelectric buoyancy.

C. Dimensionless governing equations

In the present section we introduce dimensionless numbers characterizing the considered fluid system and summarize the governing equations (7) in concise nondimensionalized form. The primary control parameter of the TEHD instability is the electric Rayleigh number L constructed as in Eq. (4). In the present problem, the averaged electric gravity is estimated as

$$G_{e,0} = \frac{2}{d} \int_0^{d/2} G_{e,b} dz = \frac{2e'\epsilon'_{\text{ref}}\Phi_0^2\gamma_e}{\rho_{\text{ref}}\alpha d^3}, \quad (19)$$

based on $G_{e,b}$ given by Eq. (18). We adopt this $G_{e,0}$ as a characteristic value of electric gravity. The definition (4) of L then reads

$$L = \frac{\alpha\Delta T G_{e,0}}{\nu\kappa} \left(\frac{d}{2}\right)^3 = \frac{\epsilon'_{\text{ref}}\epsilon_{\text{ref}}'^{1/2}e'^2\omega^2\Phi_0^6}{256\rho\nu\kappa\lambda^2}. \quad (20)$$

Half the gap width $d/2$ has been regarded as the characteristic length scale, since the temperature variation ΔT occurs over this length in the capacitor.

In the horizontal configuration of capacitor, the Archimedean thermal buoyancy affects the dynamics of fluid and brings about destabilizing effects. The significance of these effects is

characterized by the Rayleigh number Ra defined by

$$Ra = \frac{\alpha \Delta T g}{\nu \kappa} \left(\frac{d}{2} \right)^3 = \frac{\alpha \epsilon'_{\text{ref}} \tan \delta g d^3 \omega \Phi_0^2}{64 \nu \kappa \lambda}. \quad (21)$$

For a dimensionless description of the problem, these two Rayleigh numbers are supplemented by the thermoelectric parameter γ_e and by other three dimensionless numbers characterizing fluid properties: the Prandtl number $Pr = \nu/\kappa$, the loss tangent $\tan \delta$, and the ratio e_r of the two coefficients of thermal permittivity variation. For 1-nonanol, the latter three dimensionless numbers take the values $Pr = 181$, $\tan \delta = 0.0606$, and $e_r = -1.08$ at 20 °C. The parameter e_r is fixed at $e_r = -1$ throughout the present work for simplicity.

Adopting the scales d of length, d^2/κ of time, κ/d of velocity, Φ_0 of electric potential, and ΔT of temperature, we nondimensionalize the governing equations (7a)–(7e) to obtain

$$\nabla \cdot \mathbf{u} = 0, \quad (22a)$$

$$\frac{1}{Pr} \left(\frac{\partial \mathbf{u}}{\partial t} + \mathbf{u} \cdot \nabla \mathbf{u} \right) = -\nabla \pi + \nabla^2 \mathbf{u} - L\theta \mathbf{G}_e + \mathbf{f}_R + Ra\theta \mathbf{e}_z, \quad (22b)$$

$$\frac{\partial \theta}{\partial t} + \mathbf{u} \cdot \nabla \theta = \nabla^2 \theta + 8(1 - e_r \gamma_e \theta)[(\nabla \phi)^2 + (\nabla \psi)^2], \quad (22c)$$

$$\nabla^2 \phi - 2\gamma_e F_+ \theta \nabla^2 \phi - \gamma_e F_+ \nabla \theta \cdot \nabla \phi + \gamma_e F_- \nabla \theta \cdot \nabla \psi = 0, \quad (22d)$$

$$\nabla^2 \psi - 2\gamma_e F_+ \theta \nabla^2 \psi - \gamma_e F_- \nabla \theta \cdot \nabla \phi - \gamma_e F_+ \nabla \theta \cdot \nabla \psi = 0. \quad (22e)$$

The boundary conditions read as follows:

$$\mathbf{u} = 0, \quad \theta = 0, \quad \phi = 1, \quad \psi = 0, \quad \text{at } z = \frac{1}{2}, \quad (23a)$$

$$\mathbf{u} = 0, \quad \theta = 0, \quad \phi = 0, \quad \psi = 0, \quad \text{at } z = -\frac{1}{2}. \quad (23b)$$

For the momentum equation (22b), the gradient force component of $\overline{\mathbf{f}}_D$ has been lumped with the reduced pressure p_r to constitute a scalar $\pi = p_r - \epsilon'_{\text{ref}} \hat{\mathbf{E}} \cdot \hat{\mathbf{E}}^* e' \theta / 2$. It has been nondimensionalized by $\rho_{\text{ref}} (\kappa/d)^2$. The dimensionless electric gravity \mathbf{G}_e is calculated from potentials (see Appendix A for detail),

$$\mathbf{G}_e = \frac{1}{\gamma_e} \{ \nabla [(\nabla \phi)^2 + (\nabla \psi)^2] + 2e_r \tan \delta [(\nabla^2 \phi) \nabla \psi - (\nabla^2 \psi) \nabla \phi + \nabla \times (\nabla \phi \times \nabla \psi)] \}. \quad (24)$$

This expression has been obtained by substituting $\hat{\mathbf{E}} = -\nabla(\phi + i\psi)$ in Eq. (10b) and nondimensionalizing the result by the electric gravity scale $G_{e,0}$. The component \mathbf{f}_R of the DEP force is calculated as

$$\mathbf{f}_R = \frac{2L \tan \delta}{\gamma_e^2} [(\nabla^2 \phi) \nabla \psi - (\nabla^2 \psi) \nabla \phi + \nabla \times (\nabla \phi \times \nabla \psi)]. \quad (25)$$

III. LINEAR STABILITY THEORY

When the applied electric field exceeds a critical value, the base quiescent state becomes unstable and a convective flow develops in the cavity as in the Rayleigh-Bénard convection. To determine instability thresholds and the nature of growing flows, we consider a perturbed state,

$$\mathbf{u} = \tilde{\mathbf{u}}, \quad \pi = \pi_b + \tilde{\pi}, \quad \theta = \theta_b + \tilde{\theta}, \quad \phi = \phi_b + \tilde{\phi}, \quad \psi = \psi_b + \tilde{\psi}, \quad (26)$$

where perturbation fields are indicated by tildes. Linearizing Eqs. (22) around the base state $(\mathbf{u}_b, \pi_b, \theta_b, \phi_b, \psi_b)$, we obtain the following equations governing the linear dynamics of the system:

$$\nabla \cdot \tilde{\mathbf{u}} = 0, \quad (27a)$$

$$\frac{1}{\text{Pr}} \frac{\partial \tilde{\mathbf{u}}}{\partial t} = -\nabla \tilde{\pi} + \nabla^2 \tilde{\mathbf{u}} + \text{Ra} \tilde{\theta} \mathbf{e}_z + L \tilde{\theta} G_{e,b} \mathbf{e}_z - L \theta_b \tilde{\mathbf{G}}_e + \tilde{\mathbf{f}}_R, \quad (27b)$$

$$\begin{aligned} \frac{\partial \tilde{\theta}}{\partial t} = & -\frac{d\theta_b}{dz} \tilde{w} + \left[\nabla^2 - e_r \gamma_e \left(\frac{d\phi_b}{dz} \right)^2 - e_r \gamma_e \left(\frac{d\psi_b}{dz} \right)^2 \right] \tilde{\theta} \\ & + 16(1 - e_r \gamma_e \theta_b) \left(\frac{d\phi_b}{dz} \frac{\partial \tilde{\phi}}{\partial z} + \frac{d\psi_b}{dz} \frac{\partial \tilde{\psi}}{\partial z} \right), \end{aligned} \quad (27c)$$

$$\begin{aligned} \left(-2F_+ \frac{d^2 \phi_b}{dz^2} - F_+ \frac{d\phi_b}{dz} \frac{\partial}{\partial z} + F_- \frac{d\psi_b}{dz} \frac{\partial}{\partial z} \right) \tilde{\theta} + \left(\frac{1}{\gamma_e} \nabla^2 - 2F_+ \theta_b \nabla^2 - F_+ \frac{d\theta_b}{dz} \frac{\partial}{\partial z} \right) \tilde{\phi} + F_- \frac{d\theta_b}{dz} \frac{\partial \tilde{\psi}}{\partial z} \\ = 0, \end{aligned} \quad (27d)$$

$$\begin{aligned} \left(-2F_+ \frac{d^2 \psi_b}{dz^2} - F_- \frac{d\phi_b}{dz} \frac{\partial}{\partial z} - F_+ \frac{d\psi_b}{dz} \frac{\partial}{\partial z} \right) \tilde{\theta} - F_- \frac{d\theta_b}{dz} \frac{\partial \tilde{\phi}}{\partial z} + \left(\frac{1}{\gamma_e} \nabla^2 - 2F_+ \theta_b \nabla^2 - F_+ \frac{d\theta_b}{dz} \frac{\partial}{\partial z} \right) \tilde{\psi} \\ = 0. \end{aligned} \quad (27e)$$

The perturbation component $\tilde{\mathbf{G}}_e$ of the electric gravity arises from thermoelectric feedback: disturbances in temperature fields give rise to a perturbation in permittivity to modify the electric field through the Gauss law. The component $\tilde{\mathbf{f}}_R$ is a linear combination of $\tilde{\theta}$, $\tilde{\phi}$, and $\tilde{\psi}$ with coefficients involving the base field $(\theta_b, \phi_b, \psi_b)$. Explicit expressions of $\tilde{\mathbf{G}}_e$ and $\tilde{\mathbf{f}}_R$ are given in Appendix B. The solution is subject to homogeneous boundary conditions

$$\tilde{\mathbf{u}} = \mathbf{0}, \quad \tilde{\theta} = \tilde{\phi} = \tilde{\psi} = 0, \quad \text{at } z = \pm \frac{1}{2}. \quad (28)$$

We solve the complete set of linearized governing equations (27) under the boundary conditions (28) to determine the stability of the base state. This stability problem can be written formally in the following matrix representation,

$$\mathcal{A}(L, \tan \delta, \gamma_e) \tilde{\mathbf{X}} = \mathcal{B}(\text{Pr}) \frac{\partial \tilde{\mathbf{X}}}{\partial t}, \quad (29)$$

where $\tilde{\mathbf{X}} = (\tilde{\mathbf{u}} \quad \tilde{\pi} \quad \tilde{\theta} \quad \tilde{\phi} \quad \tilde{\psi})^T$. The linear operator \mathcal{A} consists of the partial derivatives with respect to the coordinates (x, y, z) and of the base flow fields $(\theta_b, \phi_b, \psi_b)$. It involves parameters $\tan \delta$, γ_e , and L . The linear operator \mathcal{B} is constant and depends only on the Prandtl number Pr .

We perform a modal analysis to determine the temporal evolution of $\tilde{\mathbf{X}}$. Since the considered capacitor system is invariant with respect to the rotation around any axis perpendicular to the electrodes, we assume a normal mode in the x - z plane: $\tilde{\mathbf{X}} = \hat{\mathbf{X}}(z) e^{st+ikx}$, without any loss of generality. We then compute the eigenvalue $s = s_r + is_i$ by applying the Chebyshev collocation method to Eq. (29). The growth rate s_r is obtained in function of the wave number k and the parameters L , Ra , Pr , $\tan \delta$, and γ_e . We vary k and the electric Rayleigh number L and determine the marginal stability curve $s_r(k, L) = 0$, keeping the other parameters constant. Seeking the value k_c of the wave number at which L on the curve attains the global minimum, we obtain the critical condition (k_c, L_c) for a given set of Ra , Pr , $\tan \delta$, and γ_e . When L exceeds the critical electric number L_c , disturbances of the critical wave number k_c grow exponentially.

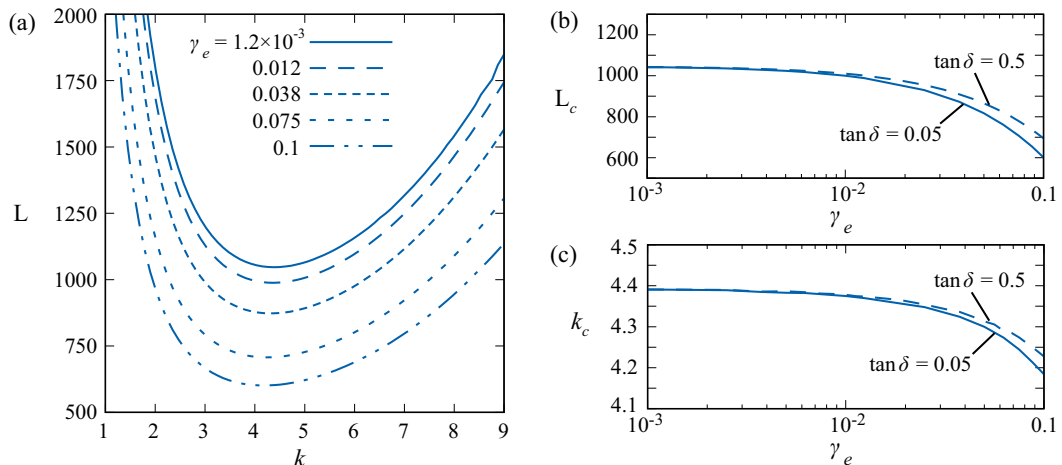


FIG. 3. The stability of the base quiescent states in microgravity environments ($Ra = 0$). (a) Marginal stability curves for some values of the thermoelectric parameter γ_e for $\tan \delta = 0.05$. (b) Critical electric Rayleigh number L_c . (c) Critical wave number k_c .

IV. RESULTS IN MICROGRAVITY ENVIRONMENTS

In the present section, we examine the convection generation by thermoelectric buoyancy only, assuming microgravity environments. The Rayleigh number Ra is fixed at $Ra = 0$. The stability depends only on the four dimensionless numbers (L , γ_e , Pr , $\tan \delta$). The analysis shows that marginal modes are stationary ($s_i = 0$). This implies that marginal stability curves and critical parameters are independent of Pr , as the Prandtl number appears only in coefficients of $\partial_t \mathbf{X}$ in the eigenvalue problem (29). The marginal and critical conditions thus vary only as functions of the thermoelectric parameter γ_e and the loss tangent $\tan \delta$. Increase of γ_e lowers marginal stability curves [Fig. 3(a)]. The critical Rayleigh and wave numbers take the values $L_c = 1047.0$ and $k_c = 4.39$ at vanishing γ_e . They decrease with γ_e when $\gamma_e > 0.01$ [Figs. 3(b) and 3(c)]. This decrease is less significant for a large loss tangent. Critical eigenmodes consist of two arrays of convection rolls (Fig. 4). Each roll occupies only half the capacitor gap. The velocity and temperature fields are symmetric with respect to the midgap plane with hot fluid flowing toward the electrodes.

The observed four-roll structure per wavelength of eigenmodes is explained from the electric gravity field $\mathbf{g}_{e,b} = -G_{e,b} \mathbf{e}_z$ and the temperature field θ_b in the base state. As discussed in Sec. II B, the base state consists of two fluid sublayers. In each of these sublayers, the density stratification is potentially unstable against the electric gravity, which changes the direction at the midgap plane of capacitor [Fig. 2(d)]. Once the thermoelectric buoyancy overcomes stabilizing diffusion effects, hot

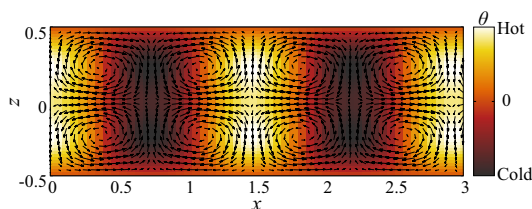


FIG. 4. The critical mode in microgravity for $\gamma_e = 0.044$ and $\tan \delta = 0.05$. The critical wave number and the electric Rayleigh number are $k_c = 4.306$ and $L_c = 844.5$.

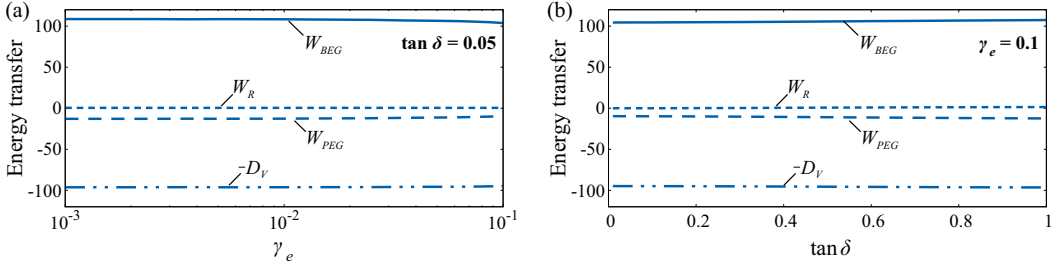


FIG. 5. Powers of different energy transfer mechanisms to perturbation flows at critical conditions [see Eq. (30)]. All the powers have been normalized by twice the flow kinetic energy K . (a) Variation of powers as a function of the thermoelectric parameter γ_e . The loss tangent is fixed at $\tan \delta = 0.05$. (b) Variation of powers as a function of $\tan \delta$. The parameter γ_e is fixed at $\gamma_e = 0.1$.

fluid “rises” against the electric gravity in each of the sublayers. Convection flow separated at the midgap plane thus develops.

The qualitative explanation of the instability mechanism in the light of the electric effective gravity can be substantiated by a consideration on energy transfer processes from the base to perturbation flows. By taking the inner product of Eq. (27b) with the perturbation flow velocity $\tilde{\mathbf{u}}$ and integrating the resulting equation in x over a wavelength and in z over the whole layer thickness, we obtain the Reynolds-Orr energy equation for the linear dynamics of perturbation flows:

$$\frac{1}{\text{Pr}} \frac{dK}{dt} = W_{BEG} + W_{PEG} + W_R - D_V, \quad (30)$$

where K is the kinetic energy of perturbation flow. The first three terms on the right-hand side are the powers of different components of the DEP force: W_{BEG} of the thermoelectric buoyancy due to the base electric gravity $\mathbf{g}_{e,b}$, W_{PEG} of the buoyancy associated with the perturbation electric gravity $\tilde{\mathbf{G}}_e$, and W_R of the DEP force component $\tilde{\mathbf{f}}_R$. The rate of viscous energy dissipation is denoted by D_V . The explicit definitions of these terms are

$$K = \left\langle \frac{\tilde{\mathbf{u}}^2}{2} \right\rangle, \quad W_{BEG} = L \langle \tilde{\theta} \tilde{w} G_{e,b} \rangle, \quad W_{PEG} = -L \langle \theta_b \tilde{\mathbf{u}} \cdot \tilde{\mathbf{G}}_e \rangle, \quad W_R = \langle \tilde{\mathbf{u}} \cdot \tilde{\mathbf{f}}_R \rangle, \\ D_V = \langle \nabla \tilde{\mathbf{u}} : (\nabla \tilde{\mathbf{u}})^T \rangle. \quad (31)$$

The angular brackets stand for the following double integral operation:

$$\langle \bullet \rangle = \int_{-1/2}^{1/2} \int_0^{2\pi/k} \bullet \, dx \, dz. \quad (32)$$

For the instability predicted by the linear stability theory, the thermoelectric buoyancy due to the base electric gravity drives thermal convection [Fig. 5(a)]. The contribution W_{PEG} of the thermoelectric feedback is always stabilizing, as observed in the previous work [21,32] on the TEHD instability in perfect dielectric fluids. The power associated with the component $\tilde{\mathbf{f}}_R$ of the DEP force is negligible in energy transfer ($W_R \approx 0$). The increase of the loss tangent does not alter the relative importance of the different energy transfer mechanisms [Fig. 5(b)]. The instability can thus be regarded as the “natural” convection in an effective electric gravity $\mathbf{G}_{e,b}$ but with significant stabilizing effects of the thermoelectric feedback.

V. RESULTS IN HORIZONTAL CAPACITORS

On the earth, the coupling of the DEP force with the thermal Archimedean buoyancy force will occur and the instability thresholds will be affected by the latter. We consider the system depicted in

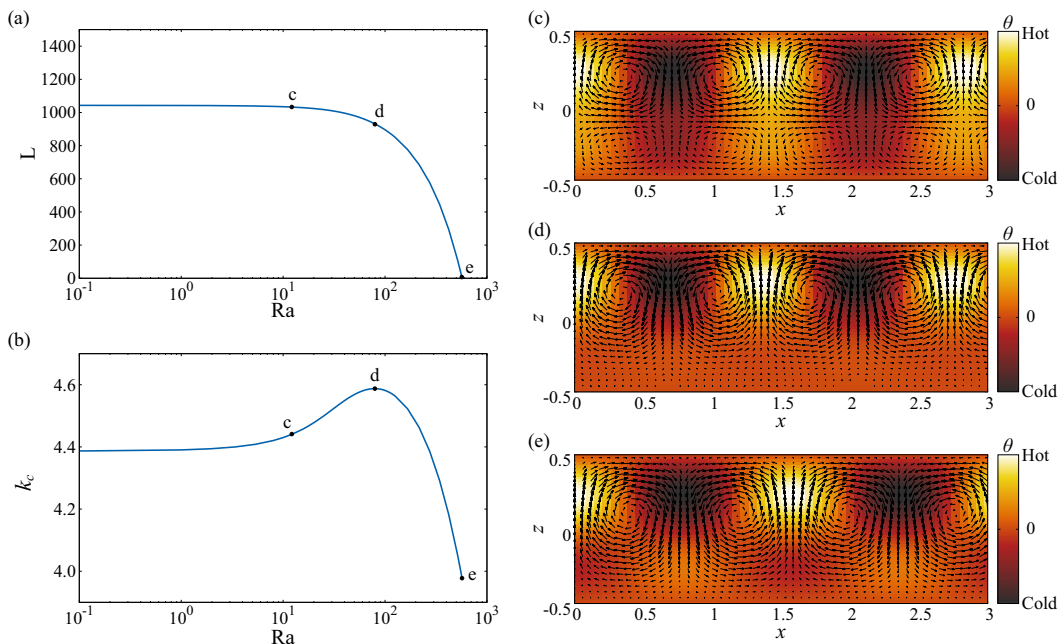


FIG. 6. Critical parameters and critical modes in a horizontal capacitor for a given loss tangent and thermoelectric parameter, $\tan \delta = 0.05$ and $\gamma_e = 0.001$. (a) Critical electric number L_c as a function of the Rayleigh number Ra . (b) Critical wave number k_c as a function of Ra . (c)–(e) Critical modes for different Ra : (c) $Ra = 12.167$, $L_c = 1032.5$, and $k_c = 4.440$; (d) $Ra = 79.507$, $L_c = 931.2$, and $k_c = 4.588$; and (e) $Ra = 569.72$, $L_c = 0$, and $k_c = 3.978$.

Fig. 1 in a horizontal configuration. The thermal and electrical conditions imposed on the capacitor are the same as those in Sec. IV, i.e., Eq. (23).

The stability of the base quiescent state could now depend on six dimensionless numbers (L , Ra , γ_e , Pr , $\tan \delta$, e_r). Stability analysis shows, however, that marginally stable modes are all stationary, so that the thresholds and critical conditions are independent of the Prandtl number as in the microgravity case. The critical electric Rayleigh number L_c decreases with the Rayleigh number Ra for $Ra \gtrsim 10$ [Fig. 6(a)]. It is vanishing as Ra approaches a value of 569.7. The variation of the critical wave number k_c is nonmonotonic [Fig. 6(b)]. It is accompanied by qualitative changes in eigenfunctions [Figs. 6(c)–6(e)]. With increasing Ra , convection rolls inside the lower half layer become weak and disappear at large Ra . This morphological change is expected from the competition between the thermoelectric and thermal Archimedean buoyancies. In the upper half layer of fluid, both the electric gravity and the earth's gravity are oriented from the top electrode to the hot core of the capacitor. So, the thermal Archimedean buoyancy provides further driving force to convection in addition to the thermoelectric buoyancy. In the lower half layer, in contrast, the earth's gravity is now directed from the hot capacitor core to the lower electrode, and the resulting thermal buoyancy impedes the convection generation. At large Ra , the stabilizing Archimedean buoyancy is dominant and the fluid motion in the lower layer is driven only by the viscous shear exerted by the convection flow developed in the upper layer.

To examine the competition between the thermoelectric and thermal Archimedean buoyancy effects quantitatively, we invoke the Reynolds-Orr equation (30) with its right-hand side completed by the power of the thermal Archimedean buoyancy force $W_G = Ra \langle \tilde{w} \tilde{\theta} \rangle$. At small Ra ($\lesssim 10$), where the critical parameters (L_c , k_c) remain constant, the thermoelectric buoyancy W_{BEG} provides energy to perturbation flows as in microgravity environments (Fig. 7). The contribution W_{PEG} of the

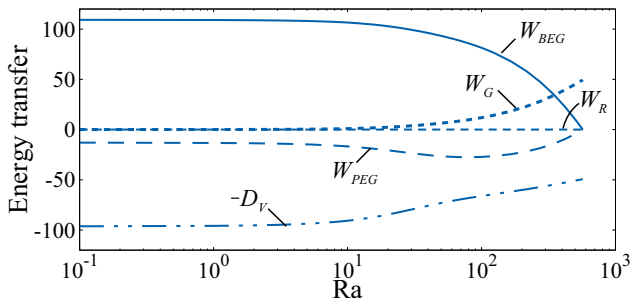


FIG. 7. Powers of different energy transfer mechanisms to perturbation flows under critical conditions in a horizontal capacitor. All the powers have been normalized by twice the flow kinetic energy K . The loss tangent and thermoelectric parameters are fixed at $\tan \delta = 0.05$ and $\gamma_e = 0.001$.

perturbation electric gravity brings about stabilizing effects. The power W_R of the force \mathbf{f}_R remains negligible. At $Ra > 10$, where L_c and k_c start decreasing, the Archimedean buoyancy effect is no longer negligible. For $Ra > 10^2$, the Archimedean buoyancy is significant. It becomes finally the dominant destabilizing mechanism when Ra is larger than 350. At $Ra = 569.72$ the instability is driven purely by the Archimedean buoyancy force.

VI. DISCUSSION

The dielectric-heating-driven TEHD instability occurs in microgravity when the electric Rayleigh number exceeds a critical value L_c with a critical eigenmode consisting of two arrays of counter-rotating convection rolls (Fig. 4). At the vanishing thermoelectric parameter γ_e , the value L_c is 1047.0 (Sec. IV), which is 2.0 times smaller than in the TEHD instability in perfect dielectric fluids in parallel plate capacitors subject to an externally imposed temperature gradient ($L_c = 2129$) [21]. This marked contrast can be explained by critical eigenfunctions. As seen in Fig. 4, the perturbation temperature has the same sign at both sides of the midgap plane separating two arrays of convection rolls. The transversal velocity gradient vanishes at the midgap plane. In this regard, this eigenmode is similar to the thermally coupled mode in the thermal convection in superposed two immiscible fluid layers [33]. This mode can develop only when two fluids have similar physical properties and similar thicknesses. Each convection roll in the double-layer system then grows under shear-free conditions at the immiscible interface. The absence of viscous shear at one side of the rolls leads to less viscous energy dissipation than in convection rolls bounded by two solid walls. For the thermally coupled mode, as a consequence, the thermal instability occurs with a critical Rayleigh number of 1101, which is identical to the value predicted for the thermal convection in a liquid layer with a nondeformable free surface [34]. This critical value is 1.6 times smaller than that of the Rayleigh-Bénard instability (1708). The reduction rate $2129/1047 \approx 2.0$ of L_c larger than 1.6 would be explained by the nonuniformity of the electric gravity in the capacitor and by the thermoelectric feedback.

In the earth's gravity environment, significant variations of the critical parameters and eigenfunctions were observed with increasing Ra (Sec. V). These variations were due to the transition from a regime dominated by the thermoelectric buoyancy to another regime dominated by the thermal Archimedean buoyancy. The results in the latter regime should agree with those reported in the literature on the thermal convection in horizontal fluid layers with internal heat generation. This problem has been studied by many researchers because of particular interests in industrial applications and in astrophysics, e.g., penetrative convection in stellar systems (see a recent review by Goluskin [35]). A particular case where the convection develops between two plates of equal temperatures has also been investigated [36,37]. In these investigations, the internal Rayleigh number Ra_{heat} based on the power density of the internal heating \mathcal{P} is often used [38]. Kulacki and Goldstein [39] performed

linear stability analyses for different boundary conditions and reported the critical values in the internal Rayleigh number $\text{Ra}_{\text{heat}} = g\alpha\mathcal{P}(d/2)^5/2\lambda\kappa\nu$, which is identical to the Rayleigh number Ra defined in Eq. (21). For uniformly heated layers between two isothermal rigid boundaries, the critical parameters reported by Kulacki and Goldstein [39] are $(k_c, \text{Ra}_{\text{heat}}) = (4.00, 583.20)$. In the present study, we obtain the critical parameters $(k_c, \text{Ra}) = (3.977, 569.7)$ for the convection driven purely by the thermal Archimedean buoyancy. This result agrees quantitatively with the results of Kulacki and Goldstein [39]. Slight differences of a few percent arise from the nonuniformity of heat generation in the present problem.

VII. CONCLUSION

We investigated the stability of stationary dielectric fluid layers subject to transversal electric fields in microgravity and in a horizontal configuration by a linear stability analysis as well as by an energetic analysis on the instability mechanism. It was shown that internal heating due to dielectric loss is able to induce convective motion in both gravitational environments. In microgravity, the convection is driven by the thermoelectric buoyancy and develops when the Rayleigh number L based on the electric effective gravity \mathbf{g}_e [Eq. (10b)] exceeds a critical value L_c . The values of L_c and of the critical wave number k_c are $L_c = 1047$ and $k_c = 4.39$ for the vanishing thermoelectric parameter γ_e . The critical conditions depend on γ_e and on the loss tangent $\tan\delta$, while they are independent of the Prandtl number Pr . The critical mode is stationary and consists of two arrays of counter-rotating convection rolls, which share common features with the thermally coupled mode in the thermal convection in horizontal double layers of immiscible fluids. That the value L_c is significantly smaller than the critical value of the TEHD instability in perfect dielectric fluids is explained by less viscous energy dissipation in convection cells arranged in two arrays. In the horizontal configuration, the critical condition varies significantly with the variation of the Rayleigh number Ra because of the competition of the electric gravity and the earth's gravity. With increasing Ra , the structure of critical modes also changes from two to single arrays of convection rolls because of increasing stabilizing effects of earth's gravity in the lower half layer of fluid. In the limit of $\text{Ra} \rightarrow 569.7$, the convection is driven purely by the thermal Archimedean buoyancy force. The critical conditions agree well with the result reported in the literature on the thermal instability of an internally heated horizontal fluid layer.

ACKNOWLEDGMENTS

The present work was performed within the framework of the LIA ISTROF (LIA 1092 CNRS). The GeoFlow research has been funded by ESA Grant No. AO-99-049, by DLR Grants No. 50WM0122, No. 50WM0822, and No. 50WM1644, and by the SOKRATES/ERASMUS program LIA-ISTROF (CNRS cooperation). C.K. and I.M. acknowledge the financial support by the CNES (French Space Agency) and the Regional Council of Normandie through the CPER-FEDER project BIOENGINE.

APPENDIX A: DIFFERENT EXPRESSIONS OF THE TIME-AVERAGED DEP FORCE

To derive Eq. (9), we introduce the unit vectors \mathbf{e}_l ($l = x, y, z$) in the Cartesian coordinate system and write the electric field and the displacement vector as $\mathbf{E} = E_l \mathbf{e}_l$ and $\mathbf{D} = D_l \mathbf{e}_l$, respectively. The Einstein's summation convention has been invoked. We define the complex amplitude $\hat{\mathbf{D}}$ of the displacement vector by $\mathbf{D} = \text{Re}[\sqrt{2} \hat{\mathbf{D}} e^{i\omega t}]$. It is related to the amplitude of the electric field as $\hat{\mathbf{D}} = (\epsilon' - i\epsilon'')\hat{\mathbf{E}}$ or, in terms of their components, $\hat{D}_l = (\epsilon' - i\epsilon'')\hat{E}_l$.

Making use of these relationships, we calculate the DEP force $\mathbf{f}_D = -(\mathbf{E}^2/2)\nabla\epsilon$ as follows:

$$\mathbf{f}_D = -\frac{E_l E_l}{2} \frac{\partial \epsilon}{\partial x_m} \mathbf{e}_m = -\frac{\partial}{\partial x_m} \left(\frac{\epsilon E_l E_l}{2} \right) \mathbf{e}_m + \frac{\epsilon}{2} \frac{\partial (E_l E_l)}{\partial x_m} \mathbf{e}_m = -\frac{\partial}{\partial x_m} \left(\frac{D_l E_l}{2} \right) \mathbf{e}_m + D_l \frac{\partial E_l}{\partial x_m} \mathbf{e}_m,$$

where we have invoked $\partial(E_l E_l)/\partial x_m = 2E_l(\partial E_l/\partial x_m)$ for the last term. The time averages of the product $D_l E_l$ over an oscillation period of electric field is calculated as

$$\begin{aligned}\overline{D_l E_l} &= \overline{\text{Re}[\sqrt{2}D_l e^{i\omega t}]\text{Re}[\sqrt{2}E_l e^{i\omega t}]} = \overline{\frac{1}{2}(\sqrt{2}\hat{D}_l e^{i\omega t} + \text{c.c.})\frac{1}{2}(\sqrt{2}\hat{E}_l e^{i\omega t} + \text{c.c.})} \\ &= \overline{\frac{1}{2}(\hat{D}_l \hat{E}_l^* + \text{c.c.})} + \overline{\frac{1}{2}(\hat{D}_l \hat{E}_l e^{i2\omega t} + \text{c.c.})} = \frac{1}{2}(\hat{D}_l \hat{E}_l^* + \text{c.c.}) \\ &= \frac{1}{2}[(\epsilon' - i\epsilon'')\hat{E}_l \hat{E}_l^* + \text{c.c.}] = \epsilon' \hat{E}_l \hat{E}_l^*,\end{aligned}$$

where c.c. means the complex conjugate of the preceding term. A similar calculation gives

$$\begin{aligned}\overline{D_l \frac{\partial E_l}{\partial x_m}} &= \frac{1}{2} \left(\hat{D}_l \frac{\partial \hat{E}_l^*}{\partial x_m} + \text{c.c.} \right) = \frac{1}{2} \left((\epsilon' - i\epsilon'') \hat{E}_l \frac{\partial \hat{E}_l^*}{\partial x_m} + \text{c.c.} \right) \\ &= \frac{\epsilon'}{2} \frac{\partial (\hat{E}_l \hat{E}_l^*)}{\partial x_m} - i \frac{\epsilon''}{2} \left(\frac{\partial \hat{E}_l^*}{\partial x_m} \hat{E}_l - \frac{\partial \hat{E}_l}{\partial x_m} \hat{E}_l^* \right).\end{aligned}$$

The time-averaged DEP force is thus given by

$$\begin{aligned}\overline{\mathbf{f}_D} &= -\frac{\partial}{\partial x_m} \left(\frac{\overline{D_l E_l}}{2} \right) \mathbf{e}_m + D_l \overline{\frac{\partial E_l}{\partial x_m}} \mathbf{e}_m \\ &= -\frac{\partial}{\partial x_m} \left(\frac{\epsilon'}{2} \hat{E}_l \hat{E}_l^* \right) \mathbf{e}_m + \frac{\epsilon'}{2} \frac{\partial (\hat{E}_l \hat{E}_l^*)}{\partial x_m} \mathbf{e}_m - i \frac{\epsilon''}{2} \left(\frac{\partial \hat{E}_l^*}{\partial x_m} \hat{E}_l - \frac{\partial \hat{E}_l}{\partial x_m} \hat{E}_l^* \right) \mathbf{e}_m \\ &= -\frac{\hat{E}_l \hat{E}_l^*}{2} \frac{\partial \epsilon'}{\partial x_m} \mathbf{e}_m - i \frac{\epsilon''}{2} \left(\frac{\partial \hat{E}_l^*}{\partial x_m} \hat{E}_l - \frac{\partial \hat{E}_l}{\partial x_m} \hat{E}_l^* \right) \mathbf{e}_m.\end{aligned}\tag{A1}$$

The last line is identical to Eq. (9).

The expression of $\overline{\mathbf{f}_D}$ in terms of potentials can be obtained by substituting $\hat{\mathbf{E}} = -(\nabla\phi + i\nabla\psi)$ in Eq. (A1). After some algebraic manipulations, we have

$$\begin{aligned}\overline{\mathbf{f}_D} &= -\frac{1}{2} \left(\frac{\partial\phi}{\partial x_l} \frac{\partial\phi}{\partial x_l} + \frac{\partial\psi}{\partial x_l} \frac{\partial\psi}{\partial x_l} \right) \frac{\partial\epsilon'}{\partial x_m} \mathbf{e}_m + \epsilon'' \left(\frac{\partial^2\phi}{\partial x_l \partial x_m} \frac{\partial\psi}{\partial x_l} - \frac{\partial^2\psi}{\partial x_l \partial x_m} \frac{\partial\phi}{\partial x_l} \right) \mathbf{e}_m \\ &= -\frac{1}{2} [(\nabla\phi)^2 + (\nabla\psi)^2] \nabla\epsilon' + \epsilon'' [(\nabla\nabla\phi) \cdot \nabla\psi - (\nabla\nabla\psi) \cdot \nabla\phi].\end{aligned}\tag{A2}$$

In the last line, $\nabla\nabla$ is a tensorial operator $\nabla\nabla = (\partial^2/\partial x_l \partial x_m) \mathbf{e}_l \mathbf{e}_m$. Making use of a mathematical identity $\nabla \times (\nabla\phi \times \nabla\psi) = \nabla^2\psi\nabla\phi - \nabla^2\phi\nabla\psi + (\nabla\nabla\phi) \cdot \nabla\psi - (\nabla\nabla\psi) \cdot \nabla\phi$, we obtain

$$\overline{\mathbf{f}_D} = -\frac{1}{2} [(\nabla\phi)^2 + (\nabla\psi)^2] \nabla\epsilon' + \epsilon'' [\nabla^2\phi\nabla\psi - \nabla^2\psi\nabla\phi + \nabla \times (\nabla\phi \times \nabla\psi)].$$

APPENDIX B: PERTURBATION COMPONENTS OF \mathbf{G}_e AND \mathbf{f}_D

The perturbation components $\tilde{\mathbf{G}}_e$ and $\tilde{\mathbf{f}}_R$ of electric gravity and the residual DEP force component are given in terms of the base states $(\theta_b, \phi_b, \psi_b)$ and the perturbation fields $(\tilde{\theta}, \tilde{\phi}, \tilde{\psi})$:

$$\begin{aligned}\tilde{\mathbf{G}}_e &= \frac{2}{\gamma_e} \left\{ \nabla \left(\frac{d\phi_b}{dz} \frac{\partial\tilde{\phi}}{\partial z} + \frac{d\psi_b}{dz} \frac{\partial\tilde{\psi}}{\partial z} \right) + e_r \tan\delta \left[\frac{d\psi_b}{dz} \nabla \left(\frac{\partial\tilde{\phi}}{\partial z} \right) - \frac{d\phi_b}{dz} \nabla \left(\frac{\partial\tilde{\psi}}{\partial z} \right) \right. \right. \\ &\quad \left. \left. + \left(\frac{d^2\phi_b}{dz^2} \frac{\partial\tilde{\psi}}{\partial z} - \frac{d^2\psi_b}{dz^2} \frac{\partial\tilde{\phi}}{\partial z} \right) \mathbf{e}_z \right] \right\},\end{aligned}$$

$$\tilde{\mathbf{f}}_R = \frac{2L \tan\delta}{\gamma_e^2} \left[\frac{d\psi_b}{dz} \nabla \left(\frac{\partial\tilde{\phi}}{\partial z} \right) - \frac{d\phi_b}{dz} \nabla \left(\frac{\partial\tilde{\psi}}{\partial z} \right) + \left(\frac{d^2\phi_b}{dz^2} \frac{\partial\tilde{\psi}}{\partial z} - \frac{d^2\psi_b}{dz^2} \frac{\partial\tilde{\phi}}{\partial z} \right) \mathbf{e}_z \right].$$

These expressions have been nondimensionalized according to the scales presented in Sec. II C.

APPENDIX C: SCALE ANALYSIS ON THERMAL BREAKDOWN

The thermal breakdown of dielectrics occurs when the internal heat generation overcomes thermal diffusion effects. This breakdown would not occur in the systems modeled in the present work, where the thermal variations of permittivities, $|e' \Delta T|$ and $|e'' \Delta T|$, are assumed to be small for the validity of Eq. (8). The present Appendix aims to clarify this point.

For a perturbation in temperature $\delta\theta$, corresponding perturbations in the heat generation density and in the thermal diffusion are

$$\delta\overline{P_D} \sim \delta(\omega\epsilon''E^2) \sim \omega\epsilon''E^2 \left(\frac{\delta\epsilon''}{\epsilon''} + \frac{2\delta E}{E} \right) \sim \omega E^2 \delta\epsilon'' \sim -\omega E^2 \epsilon''_{\text{ref}} e'' \delta\theta, \quad (\text{C1})$$

$$\delta(\lambda \nabla^2 T) \sim \lambda \frac{\delta\theta}{d^2}, \quad (\text{C2})$$

where the symbol δ is used to indicate the perturbation of the succeeding term. The scaling relationship $\delta E/E \sim \delta\epsilon''/\epsilon''$, derived from Gauss' law, and Eq. (8) have been invoked. The criterion of the thermal breakdown $\delta\overline{P_D} \gtrsim \delta(\lambda \nabla^2 T)$ then reads

$$\frac{\delta\overline{P_D}}{\delta(\lambda \nabla^2 T)} \sim |e''| \frac{\omega\epsilon''_{\text{ref}} E^2 d^2}{\lambda} \sim |e''| \Delta T \gtrsim 1, \quad (\text{C3})$$

where we have made use of the relationship $\omega\epsilon''_{\text{ref}} E^2 d^2 / \lambda \Delta T \approx 1$ (see Sec. II B). The criterion (C3) is never satisfied by systems considered in the present work.

-
- [1] J. R. Melcher, *Continuum Electromechanics* (MIT, Cambridge, MA, 1981).
 - [2] A. Castellanos, Editor, *Electrohydrodynamics* (Springer-Verlag, Wien, 1998).
 - [3] T. B. Jones, Electrohydrodynamically enhanced heat transfer in liquids—A review, [Adv. Heat Transfer **14**, 107 \(1979\)](#).
 - [4] T. B. Jones, *Electromechanics of Particles* (Cambridge University, Cambridge, England, 2005).
 - [5] J. Deval, P. Tabeling, and C.-M. Ho, A dielectrophoretic chaotic mixer, in *Technical Digest, Fifteenth IEEE International Conference on Micro Electro Mechanical Systems, Las Vegas, NV* (IEEE, Piscataway, NJ, 2002), pp. 36–39.
 - [6] L. D. Landau and E. M. Lifshitz, *Electrodynamics of Continuous Media*, 2nd ed., Landau and Lifshitz Course of Theoretical Physics, Vol. 8 (Butterworth-Heinemann, Burlington, MA, 1984).
 - [7] P. J. Stiles, Electro-thermal convection in dielectric liquids, [Chem. Phys. Lett. **179**, 311 \(1991\)](#).
 - [8] B. Futterer, A. Krebs, A.-C. Plesa, F. Zaussinger, R. Hollerbach, D. Breuer, and C. Egbers, Sheet-like and plume-like thermal flow in a spherical convection experiment performed under microgravity, [J. Fluid Mech. **735**, 647 \(2013\)](#).
 - [9] P. H. Roberts, Electrohydrodynamic convection, [Q. J. Mech. Appl. Math. **22**, 211 \(1969\)](#).
 - [10] R. J. Turnbull, Effect of dielectrophoretic forces on the Bénard instability, [Phys. Fluids **12**, 1809 \(1969\)](#).
 - [11] B. Chandra and D. E. Smylie, A laboratory model of thermal convection under a central force field, [Geophys. Fluid Dyn. **3**, 211 \(1972\)](#).
 - [12] I. M. Yavorskaya, N. I. Fomina, and Yu. N. Belyaev, A simulation of central-symmetry convection in microgravity conditions, [Acta Astronaut. **11**, 179 \(1984\)](#).
 - [13] J. E. Hart, G. A. Glatzmaier, and J. Toomre, Space-laboratory and numerical simulations of thermal convection in a rotating hemispherical shell with radial gravity, [J. Fluid Mech. **173**, 519 \(1986\)](#).
 - [14] A. Meyer, M. Jongmanns, M. Meier, Ch. Egbers, and I. Mutabazi, Thermal convection in a cylindrical annulus under a combined effect of the radial and vertical gravity, [C. R. Mécanique **345**, 11 \(2017\)](#).
 - [15] Ch. Egbers, W. Beyer, A. Bonhage, R. Hollerbach, and P. Beltrame, The geoflow-experiment on ISS (part I): Experimental preparation and design of laboratory testing hardware, [Adv. Space Res. **32**, 171 \(2003\)](#).
 - [16] F. Zaussinger, A. Krebs, V. Travnikov, and Ch. Egbers, Recognition and tracking of convective flow patterns using Wollaston shearing interferometry, [Adv. Space Res. **60**, 1327 \(2017\)](#).

- [17] F. Feudel, K. Bergemann, L. S. Tuckerman, C. Egbers, B. Futterer, M. Gellert, and R. Hollerbach, Convection patterns in a spherical fluid shell, *Phys. Rev. E* **83**, 046304 (2011).
- [18] V. Travnikov, F. Zaussinger, P. Beltrame, and C. Egbers, Influence of the temperature-dependent viscosity on convective flow in the radial force field, *Phys. Rev. E* **96**, 023108 (2017).
- [19] F. Zaussinger, P. Canfield, A. Froitzheim, V. Travnikov, P. Haun, M. Meier, A. Meyer, P. Heintzmann, T. Driebe, and Ch. Egbers, AtmoFlow—Investigation of atmospheric-like fluid flows under microgravity conditions, *Microgravity Sci. Technol.* **31**, 569 (2019).
- [20] A. Meyer, O. Crumeyrolle, I. Mutabazi, M. Meier, M. Jongmanns, M.-C. Renoult, T. Seelig, and Ch. Egbers, Flow patterns and heat transfer in a cylindrical annulus under 1g and low-g conditions: Theory and simulation, *Microgravity Sci. Technol.* **30**, 653 (2018).
- [21] H. N. Yoshikawa, M. Tadie Fogaing, O. Crumeyrolle, and I. Mutabazi, Dielectric Rayleigh-Bénard convection under microgravity conditions, *Phys. Rev. E* **87**, 043003 (2013).
- [22] F. Zaussinger, P. Haun, M. Neben, T. Seelig, V. Travnikov, Ch. Egbers, H. N. Yoshikawa, and I. Mutabazi, Dielectrically driven convection in spherical gap geometry, *Phys. Rev. Fluids* **3**, 093501 (2018).
- [23] V. Travnikov, F. Zaussinger, P. Haun, and Ch. Egbers, Influence of dielectrical heating on convective flow in a radial force field, *Phys. Rev. E* **101**, 053106 (2020).
- [24] F. Zaussinger, P. Haun, P. S. B. Szabo, V. Travnikov, M. Al Kawwas, and C. Egbers, Rotating spherical gap convection in the GeoFlow International Space Station (ISS) experiment, *Phys. Rev. Fluids* **5**, 063502 (2020).
- [25] B. Futterer, N. Dahley, S. Koch, N. Scurtu, and C. Egbers, From viscous convective experiment ‘GeoFlow I’ to temperature-dependent viscosity in ‘GeoFlow II’—Fluid physics experiments on-board ISS for the capture of convection phenomena in Earth’s outer core and mantle, *Acta Astronaut.* **71**, 11 (2012).
- [26] J. R. Melcher and G. I. Taylor, Electrohydrodynamics: A review of the role of interfacial shear stresses, *Annu. Rev. Fluid Mech.* **1**, 111 (1969).
- [27] D. A. Saville, Electrohydrodynamics: The Taylor-Melcher leaky dielectric model, *Annu. Rev. Fluid Mech.* **29**, 27 (1997).
- [28] A. I. Zhakin, Electrohydrodynamics, *Phys.-Usp.* **55**, 465 (2012).
- [29] B. L. Smorodin, The effect of an alternating electric field on the liquid dielectric convection in a horizontal capacitor, *Tech. Phys. Lett.* **27**, 1062 (2001).
- [30] B. L. Smorodin and M. G. Velarde, On the parametric excitation of electrothermal instability in a dielectric liquid layer using an alternating electric field, *J. Electrostat.* **50**, 205 (2001).
- [31] E. Kuffel, W. S. Zaengl, and J. Kuffel, *High Voltage Engineering Fundamentals*, 2nd ed. (Butterworth-Heinemann, Burlington, MA, 2000).
- [32] H. N. Yoshikawa, O. Crumeyrolle, and I. Mutabazi, Dielectrophoretic force-driven thermal convection in annular geometry, *Phys. Fluids* **25**, 024106 (2013).
- [33] S. Rasenat, F. H. Busse, and I. Rehberg, A theoretical and experimental study of double-layer convection, *J. Fluid Mech.* **199**, 519 (1989).
- [34] A. Pellew and R. V. Southwell, On maintained convective motion in a fluid heated from below, *Proc. R. Soc. London, Ser. A* **176**, 312 (1940).
- [35] D. Goluskin, *Internally Heated Convection and Rayleigh-Bénard Convection* (Springer, Berlin, 2016).
- [36] J. M. Straus, Penetrative convection in a layer of fluid heated from within, *Astro. Phys. J.* **209**, 179 (1976).
- [37] D. Goluskin and E. P. van der Poel, Penetrative internally heated convection in two and three dimensions, *J. Fluid Mech.* **791**, R6 (2016).
- [38] P. H. Roberts, Convection in horizontal layers with internal heat generation, *J. Fluid Mech.* **30**, 33 (1967).
- [39] F. A. Kulacki and R. J. Goldstein, Hydrodynamic instability in fluid layers with uniform volumetric energy sources, *Appl. Sci. Res.* **31**, 81 (1975).